



## RESEARCH ARTICLE

## PALEOECOLOGY

# Oldest evidence of abundant C<sub>4</sub> grasses and habitat heterogeneity in eastern Africa

Daniel J. Peppe<sup>1†</sup>, Susanne M. Cote<sup>2†</sup>, Alan L. Deino<sup>3</sup>, David L. Fox<sup>4†</sup>, John D. Kingston<sup>5†</sup>, Rahab N. Kinyanjui<sup>6,7,8</sup>, William E. Lukens<sup>9†</sup>, Laura M. MacLatchy<sup>5,10†</sup>, Alice Novello<sup>11,12†</sup>, Caroline A. E. Strömberg<sup>12†</sup>, Steven G. Driese<sup>1</sup>, Nicole D. Garrett<sup>13</sup>, Kayla R. Hillis<sup>14</sup>, Bonnie F. Jacobs<sup>15</sup>, Kirsten E. H. Jenkins<sup>16</sup>, Robert M. Kityo<sup>17</sup>, Thomas Lehmann<sup>18</sup>, Fredrick K. Manthi<sup>6</sup>, Emma N. Mbua<sup>6</sup>, Lauren A. Michel<sup>14</sup>, Ellen R. Miller<sup>19</sup>, Amon A. T. Mugume<sup>17,20</sup>, Samuel N. Muteti<sup>6,13</sup>, Isaiah O. Nengo<sup>21,22§</sup>, Kennedy O. Oginga<sup>1¶</sup>, Samuel R. Phelps<sup>23#</sup>, Pratiqya Polissar<sup>24</sup>, James B. Rossie<sup>22</sup>, Nancy J. Stevens<sup>25</sup>, Kevin T. Uno<sup>26</sup>, Kieran P. McNulty<sup>13\*†</sup>

The assembly of Africa's iconic C<sub>4</sub> grassland ecosystems is central to evolutionary interpretations of many mammal lineages, including hominins. C<sub>4</sub> grasses are thought to have become ecologically dominant in Africa only after 10 million years ago (Ma). However, paleobotanical records older than 10 Ma are sparse, limiting assessment of the timing and nature of C<sub>4</sub> biomass expansion. This study uses a multiproxy design to document vegetation structure from nine Early Miocene mammal site complexes across eastern Africa. Results demonstrate that between ~21 and 16 Ma, C<sub>4</sub> grasses were locally abundant, contributing to heterogeneous habitats ranging from forests to wooded grasslands. These data push back the oldest evidence of C<sub>4</sub> grass-dominated habitats in Africa—and globally—by more than 10 million years, calling for revised paleoecological interpretations of mammalian evolution.

Grasses using the C<sub>4</sub> photosynthetic pathway are ubiquitous across Earth's low to mid-latitudes, dominating modern tropical lowland grassland and savannah ecosystems. C<sub>4</sub> grassy biomes play an important role in regulating global climate and have been linked to key adaptations and diversification in mammalian faunas (1–3). The C<sub>4</sub> photosynthetic pathway is physiologically advantageous under conditions of aridity, higher temperatures and irradiance, seasonal climates, and low atmospheric partial pressure of carbon dioxide (pCO<sub>2</sub>) (1). Phylogenetic analyses show that, beginning in the Paleocene, C<sub>4</sub> photosynthesis evolved independently at least 21 times from C<sub>3</sub> ancestors within the generally warm-adapted and shade-tolerant PACMAD (Panicoidae, Arundinoideae, Chloridoideae, Micrairoideae, Aristidoideae, Danthonioideae) grass clade (2). However, such ancient origins are not corroborated by the geologic record. Likewise, abundant C<sub>4</sub> biomass, for which we use a working definition of ≥30% C<sub>4</sub> biomass, is not documented before ~10 million years ago (Ma), except in isolated cases (4–6). Instead, major ecological shifts from C<sub>3</sub> vegetation to C<sub>4</sub> grasslands are well documented regionally and globally between 10 and 1 Ma (2, 3, 7, 8). This apparent contradiction between phylogenetic estimates and geological evidence of C<sub>4</sub> emergence times has confounded attempts to explain the origins and global spread of C<sub>4</sub> grasslands (2, 3, 9).

Within eastern Africa, the expansion of C<sub>4</sub> grasslands has been intensely studied because of their relevance for interpreting the evolu-

tion of numerous mammalian lineages, including the hominin clade. Carbon isotope data from multiple substrates suggest that ecologically important C<sub>4</sub> biomass appeared in the region only after 10 Ma (8, 10–13). However, older vegetation records are sparse (14, 15). This paucity of data from the Paleogene and early Neogene has led to inferences that equatorial Africa was largely forested, with C<sub>4</sub> grasses and open habitats making up only minor elements of the landscape until the Late Miocene (4, 7, 11).

Here, we present a multiproxy study of Early Miocene fossil mammal site complexes in Kenya and Uganda (Fig. 1) that combines carbon isotope analyses of bulk soil organic matter, plant wax biomarkers, and pedogenic carbonates with inferences from phytolith (microscopic plant silica body) assemblages, forming a comprehensive approach to paleoecological reconstruction (16). Specifically, we assess the role of grasses, especially C<sub>4</sub> grasses, in early Neogene habitats of eastern Africa.

## Early Miocene habitat heterogeneity, open habitats, and locally abundant C<sub>4</sub> vegetation

Results from carbon isotope analyses of ancient soil organic matter at these sites demonstrate a surprisingly high degree of habitat heterogeneity, with most datasets yielding δ<sup>13</sup>C values that reflect vegetation types ranging from closed canopy to wooded grassland, and no clear trends toward increasing or decreasing openness through time in the Early Miocene or spatially across eastern Africa (Fig. 2A and data S1) (16). Every site yielded some paleosol

samples with δ<sup>13</sup>C values indicating that soil organic biomass was a mixture of C<sub>3</sub> plants and water-stressed C<sub>3</sub> and/or C<sub>4</sub> biomass (Fig. 2A) (16, 17). Soil organic matter δ<sup>13</sup>C values at Moroto, Tinderet, Bukwa, Rusinga, and Karungu reflect more open values that extend into the range of modern woodlands, bushlands, and shrublands, with Moroto, Bukwa, and Rusinga indicating a proportion of C<sub>4</sub> biomass equivalent to those characterizing extant wooded grasslands (Fig. 2A). Taken together, we interpret these results to reflect regionally abundant C<sub>4</sub> grasses that were heterogeneously present on the landscape.

Interpreting ancient soil organic matter δ<sup>13</sup>C values is complicated by potential preferential degradation of isotopically light, labile components and by higher rates of decomposition of C<sub>4</sub>-derived carbon observed in mixed C<sub>3</sub>-C<sub>4</sub> systems (16, 18). Furthermore, although the carbon in soil organic matter predominantly

<sup>1</sup>Department of Geosciences, Baylor University, Waco, TX 76798, USA. <sup>2</sup>Department of Anthropology and Archaeology, University of Calgary, Calgary, AB T2N 1N4, Canada. <sup>3</sup>Berkeley Geochronology Center, Berkeley, CA 94709, USA. <sup>4</sup>Department of Earth and Environmental Sciences, University of Minnesota, Minneapolis, MN 55455, USA. <sup>5</sup>Department of Anthropology, University of Michigan, Ann Arbor, MI 48109, USA. <sup>6</sup>Department of Earth Sciences, National Museums of Kenya, Nairobi 00100, Kenya. <sup>7</sup>Max Planck Institute for Geoanthropology, D-07743 Jena, Germany. <sup>8</sup>Human Origins Program, National Museum of Natural History, Smithsonian Institution, Washington, DC 20013, USA. <sup>9</sup>Department of Geology & Environmental Science, James Madison University, Harrisonburg, VA 22807, USA. <sup>10</sup>Museum of Paleontology, University of Michigan, Ann Arbor, MI 48109, USA. <sup>11</sup>CEREGE, Aix-Marseille Université, CNRS, IRD, Collège de France, INRAE, 13545 Aix en Provence, France. <sup>12</sup>Department of Biology, Burke Museum of Natural History and Culture, University of Washington, Seattle, WA 98195, USA. <sup>13</sup>Department of Anthropology, University of Minnesota, Minneapolis, MN 55455, USA. <sup>14</sup>Department of Earth Sciences, Tennessee Tech University, Cookeville, TN 38505, USA. <sup>15</sup>Roy M. Huffington Department of Earth Sciences, Southern Methodist University, Dallas, TX 75275, USA. <sup>16</sup>Department of Social Sciences, Tacoma Community College, Tacoma, WA 98466, USA. <sup>17</sup>Department of Zoology Entomology and Fisheries Sciences, Makerere University, Kampala, Uganda. <sup>18</sup>Department Messel Research and Mammalogy, Senckenberg Research Institute and Natural History Museum, 60325 Frankfurt, Germany. <sup>19</sup>Department of Anthropology, Wake Forest University, Winston-Salem, NC 27109, USA. <sup>20</sup>Uganda National Museum, Department of Museums and Monuments, Ministry of Tourism, Wildlife and Antiquities, Kampala, Uganda. <sup>21</sup>Turkana Basin Institute, Stony Brook University, Stony Brook, NY 11794, USA. <sup>22</sup>Department of Anthropology, Stony Brook University, Stony Brook, NY 11794, USA. <sup>23</sup>Department of Earth and Planetary Sciences, Harvard University, Cambridge, MA 02138, USA. <sup>24</sup>Ocean Sciences Department, University of California, Santa Cruz, Santa Cruz, CA 95064, USA. <sup>25</sup>Department of Biomedical Sciences, Heritage College of Osteopathic Medicine, and Ohio Center for Ecological and Evolutionary Studies, Ohio University, Athens, OH 45701, USA. <sup>26</sup>Division of Biology and Paleo Environment, Lamont-Doherty Earth Observatory of Columbia University, Palisades, NY 10964, USA.

\*Corresponding author. Email: kmcnulty@umn.edu

†These authors contributed equally to this work.

#Present address: Aix-Marseille Université, Direction de la Recherche et de la Valorisation, 13001 Marseille, France.

§Deceased. ¶Present address: Terra Guidance, Englewood, CO 80110, USA. #Present address: CIM Group, New York, NY 10022, USA.

comes from bulk plant material, it can also come from soil microbiota, mycorrhizae, or fungi. However, long-chain *n*-alkanes are a single, plant-derived molecule, and our  $\delta^{13}\text{C}$  values from leaf wax *n*-alkanes extracted from the

same samples as soil organic matter yielded parallel results: substantial variation within stratigraphic sections and abundant  $\text{C}_4$  biomass at Moroto and Rusinga (Fig. 2B, figs. S1 and S2, and data S2 and S3) (16). The  $\text{C}_{31}$  *n*-

alkane includes input from both woody and grassy vegetation, so moderate  $\delta^{13}\text{C}$  values for this homolog cannot unequivocally distinguish low concentrations of  $\text{C}_4$  biomass from water-stressed  $\text{C}_3$  biomass (8, 16). However, the  $\text{C}_{35}$  *n*-alkane is preferentially produced by  $\text{C}_4$  grasses (19), therefore samples at Moroto with high  $\delta^{13}\text{C}$  values in both  $\text{C}_{35}$  and  $\text{C}_{31}$  *n*-alkanes unambiguously indicate considerable  $\text{C}_4$  biomass (Fig. 2B and fig. S1) (20). In addition, the high relative abundance of long-chain *n*-alkanes ( $\text{C}_{33}$  and  $\text{C}_{35}$ ) from Moroto is similar to patterns found in modern  $\text{C}_4$  grasslands (19) and in sediments from  $\text{C}_4$ -dominated environments (fig. S1) (21). Interestingly, *n*-alkane  $\delta^{13}\text{C}$  values from marine cores off of western and eastern African coasts do not provide evidence of regionally abundant Early Miocene  $\text{C}_4$  vegetation (8, 10, 11). This apparent discrepancy likely reflects differences in scale and resolution between paleosols sampled in this study, which represent local vegetation, and sediments deposited at deep-sea marine core sites, which integrate plant wax carbon isotope records over thousands of square kilometers.

Pedogenic carbonate isotopic values confirm variation within and among sites. Pedogenic carbonate was not found at all sites, nor uniformly throughout sections where it was present (16), demonstrating spatial and temporal variation in climate (i.e., mesic conditions) and/or pedogenic processes (e.g., acidic pH) that inhibited carbonate precipitation. Carbonate  $\delta^{13}\text{C}$  distributions are shifted even more toward open habitats relative to organic matter (Fig. 2C and data S4) (16), with a few  $\delta^{13}\text{C}$  values indicating  $\text{C}_4$ -dominated vegetation for some paleosols at multiple sites (Moroto, Napak, Karungu, and Buluk). Bulk soil organic matter

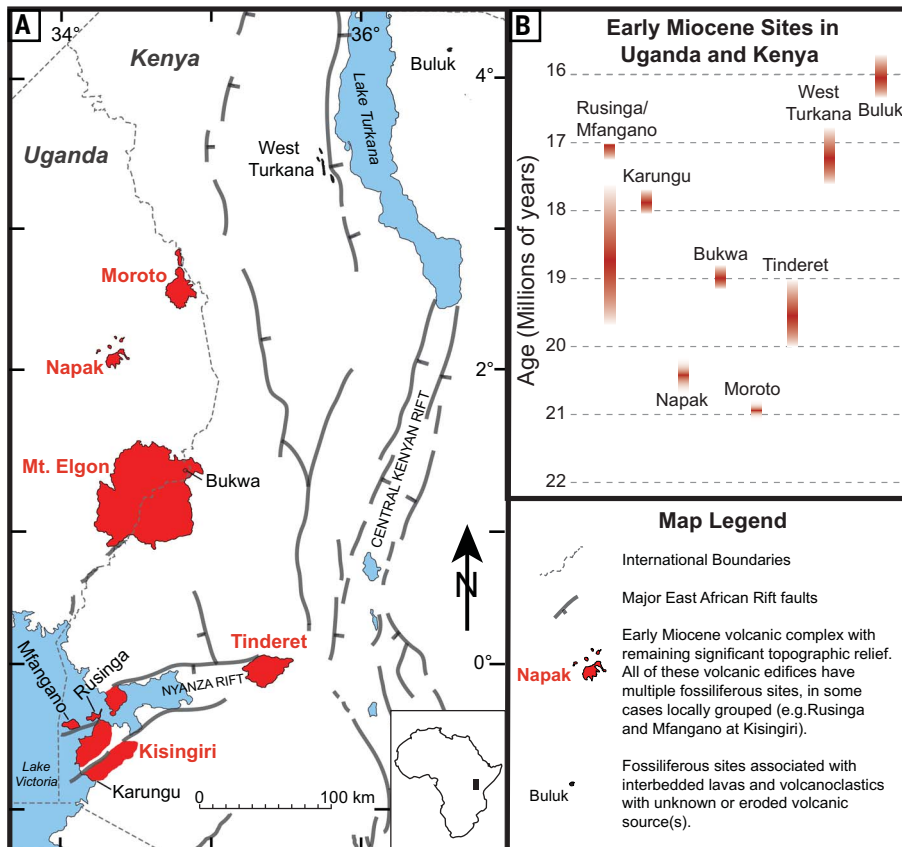
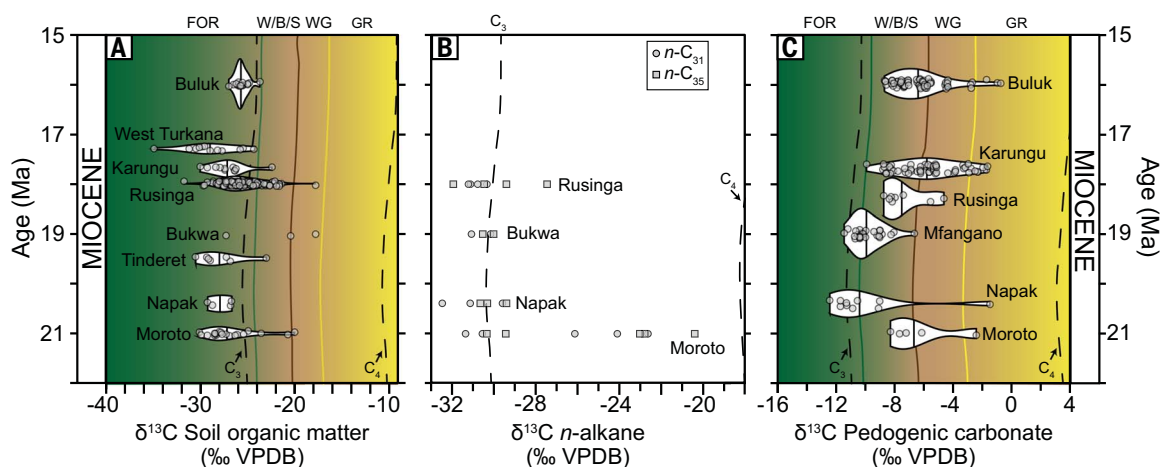


**Fig. 1. Early Miocene fossil site complexes in eastern Africa.** (A) Map of sites. Areas in red represent current exposures of primarily volcanic and associated sedimentary rock. (B) Chronology of fossil sites sampled. Further site information is provided in the supplementary materials (16).

## Fig. 2. Stable carbon isotope ratios ( $\delta^{13}\text{C}$ ) for three proxies.

(A) Bulk soil organic matter, (B)  $\text{C}_{31}$  and  $\text{C}_{35}$  *n*-alkane homologs, and (C) pedogenic carbonates. Data distributions in (A) and (C) shown as violin plots (mirrored kernel density estimates), with violin areas normalized in each panel and trimmed to data ranges in each group; points are jittered for clarity, and vertical crossbars



indicate the median of the group. Dashed lines represent mean  $\text{C}_3$  and  $\text{C}_4$  endmember  $\delta^{13}\text{C}$  values for soil organic matter and pedogenic carbonates (34) and *n*-alkanes (11) based on data from modern soils; shaded regions with colored boundaries represent UNESCO biome classifications after (35). Biome boundaries for *n*-alkanes have not been sufficiently characterized and thus are not shown. Endmembers and biome boundaries have been corrected for Miocene atmospheric  $\text{CO}_2$   $\delta^{13}\text{C}$  value after (36). Detailed methodology and data are provided in (16) and tables S1 and S2 and data S1, S2, and S4. VPDB, Vienna Pee Dee belemnite; FOR, forest; W/B/S, woodland/bushland/shrubland; WG, woody grassland; GR, grassland.

and carbonate  $\delta^{13}\text{C}$  values from the same stratigraphic levels are not significantly correlated (fig. S3B), and the mean offset between them [ $\Delta^{13}\text{C}_{\text{CO}_3\text{-OM}} = 20.0$  per mil (‰)] is greater than theoretical expectations (~14 to 17‰) (22), possibly indicating that pedogenic carbonates or organic matter (or both) do not preserve original environmental signatures. This interpretation is unlikely for several reasons. First, samples with matched soil organic matter and *n*-alkane  $\delta^{13}\text{C}$  values show strong, significant correlations (Fig. 2, A and B, and fig. S3), supporting the fidelity of the isotopic signals from our larger bulk organic dataset. Second, our field sampling strategy involved collection of pedogenic carbonates well within the subsoil, typically at least 0.5 m in depth, on the basis of the description of paleosol horizonation and macroscopic pedogenic morphologies (16) (data S4). Third, the carbonates used for paleovegetation reconstruction were pre-

pared by drilling micritic crystal textures on cut and polished rock samples after petrographic analysis, including cathodoluminescence petrography, whenever possible (16). We also purposefully sampled sparry carbonate in addition to pedogenic micrite to assess for diagenetic contamination (fig. S4). However, we found no correspondence between crystal texture and either  $\delta^{13}\text{C}$  or  $\delta^{15}\text{O}$  values (fig. S5) (16), from which we infer that diagenesis cannot account for  $\delta^{13}\text{C}$  values above a  $\text{C}_3$  endmember threshold. Fourth, paleosol morphologies and reconstructed hydroclimate from independent proxies at multiple sites (6, 20, 23) are consistent with high soil respiration rates, minimizing the possibility that infiltration of atmospheric  $\text{CO}_2$  into soil profiles drove the elevated carbonate  $\delta^{13}\text{C}$  values that we measured.

We propose instead that both pedogenic carbonates and soil organic matter preserve environmental signals that capture different

components of floral compositions at different time resolutions. Many paleosols that we sampled were deposited and formed in dynamic, aggradational landscapes associated with rifting and volcanism (20, 23), which would have caused short-term local changes in the composition of vegetation as the plant community responded to frequent disturbances. Owing to faster humus turnover times relative to the pace of carbonate accumulation (24), soil organic matter would retain the last phase of vegetation for any one profile, yet carbonates would capture a longer-term, but seasonally biased, signal of respired  $\text{CO}_2$ , reflecting vegetation that was most productive during warm and dry seasons (i.e.,  $\text{C}_4$  plants). Consequently, carbonates would be more sensitive to recording  $\text{C}_4$  plant presence compared with bulk organic matter from the same paleosols, especially if net primary productivity were higher in wetter seasons with more  $\text{C}_3$  biomass.

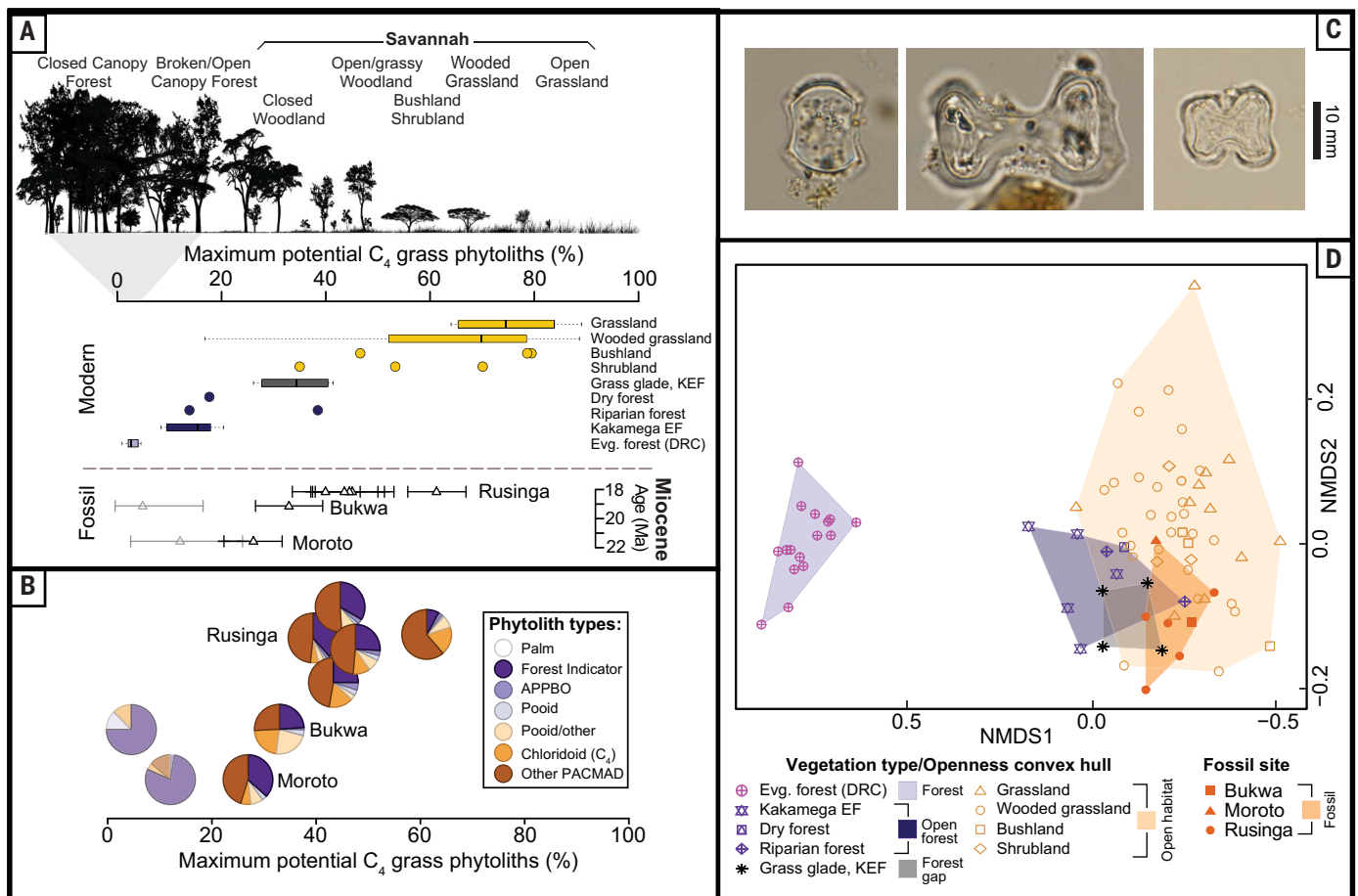


**Fig. 3. Comparison of phytolith assemblages from fossil sites and modern vegetation types in eastern and central Africa. (A)** Maximum potential  $\text{C}_4$  (i.e., PACMAD) grass phytoliths of diagnostic counts from modern vegetation types (top; showing median and quartiles for types with more than four data points) and fossil sites (bottom; showing bootstrapped 95% confidence intervals around estimates). Light-gray fossil ranges represent assemblages with low diagnostic counts. **(B)** Pie charts representing diagnostic assemblage data (excluding nondiagnostic grass phytoliths). Sites are arranged stratigraphically, and ages for

sites are shown in (A) and Fig. 1. Faded pie charts as in (A). **(C)** Representative PACMAD grass phytolith types from left to right: SADDLE ( $\text{C}_4$  Chloridoideae), BILOBATE (PACMAD), and CROSS (PACMAD). **(D)** Ordination [nonmetric multidimensional scaling (NMDS);  $k = 2$ ] of modern and fossil assemblage data. Details and data are provided in (16) and data S5 to S11. **APPBO, closed-habitat grasses, which are diagnostic of early diverging grasses in the families Anomochloideae, Pharoideae, Puelioideae, Bambusoideae, and Oryzoideae;** DRC, Democratic Republic of Congo; Evg. forest or EF, evergreen forest; KEF, Kakamega evergreen forest.

The ecological significance of  $C_4$  grasses and habitat heterogeneity is further corroborated by phytolith assemblages documenting vegetation on these Early Miocene landscapes (16). Every site that yielded phytoliths provided evidence of grasses, and all except Napak and Moruorot had phytoliths from PACMAD grasses (i.e., potential  $C_4$  grasses) (data S5 and S6). Well-preserved assemblages from Moroto, Bukwa, and Rusinga could be analyzed quantitatively, and most are dominated by grass phytoliths (up to 91.9% of diagnostic phytolith counts; Fig. 3A, fig. S6, and data S5) (16). As many as 90.8% of grass phytoliths (excluding unknown and damaged forms) are diagnostic of PACMADs, and up to 29.0% of grass phytoliths are typical of the strictly- $C_4$  Chloridoideae PACMAD subclade (Fig. 3B). Nonchloridoid PACMAD phytoliths could represent  $C_3$  or  $C_4$  grasses, but strong  $C_4$  isotopic signals from the same sites suggest that many derived from  $C_4$  species. Nevertheless, to acknowledge this inherent uncertainty, we refer to the sum of PACMAD phytoliths as “maximum potential  $C_4$  phytoliths” (Figs. 3A and 4). Consistent with isotopic evidence for habitat heterogeneity, the relative abundance of forest indicator phytoliths varied within and across sites as well, ranging from 8.1 to 81.8% (Fig. 3A and data S5).

Proportions of potential  $C_4$  grasses in fossil phytolith assemblages most closely resemble modern eastern and central African habitats with substantial grass components: wooded grasslands, shrubland, bushland, riparian forests, and grassy glades within forests (Fig. 3A). Early Miocene grass communities were diverse, including phytoliths typical of closed-habitat grasses, various PACMAD grasses (Fig. 3, B and C), and potentially Pooideae grasses (strictly  $C_3$ ) (table S5). Nonmetric multidimensional scaling distinguishes closed habitats, represented by the Guineo-Congolian lowland rainforest, from open habitats in the form of (wooded) grasslands, shrublands, and bushlands (Fig. 3D, fig. S7, and table S1) (16). Assemblages from forests with substantial grassy glades (i.e., Kakamega) or that are surrounded by open, grass-dominated vegetation (i.e., riparian forests in savannah landscapes) partly overlap with open, grassy vegetation types, but most Early Miocene assemblages fall outside these compositional fields, instead showing greater similarity with  $C_4$  grass-dominated habitats.

Together, our data from multiple chronologically constrained paleoecological proxies reveal that: (i)  $C_4$  grasses were present in the Early Miocene of eastern Africa, and at some sites were a dominant part of the vegetation;

(ii) open habitats (e.g., woodland, bushland, shrubland, and wooded grassland biomes) were a substantial and important component of Early Miocene ecosystems, contributing to landscape heterogeneity at individual sites and across the region both spatially and temporally (Figs. 3 and 4, and fig. S8); and (iii) the range of habitats and  $\delta^{13}C$  values (Fig. 4, A to D, and fig. S8) and the  $C_4$  grass abundances (Fig. 3, A and B) during the Early Miocene were at times similar to grassy savannah and woodland ecosystems reconstructed for the Late Miocene and Plio-Pleistocene (Fig. 4, A to D, and fig. S8) (25), only lacking evidence of true grasslands or rainforests [but see (26)]. Although it remains a challenge to differentiate spatial and temporal heterogeneity at a local level because our paleosol and paleoecological proxies are time-averaged to various degrees, temporally restricted horizons at Moroto and Rusinga document penecontemporaneous forested to grassy woodland microhabitats (20, 23), suggesting that landscape-scale spatial heterogeneity contributed to the variable paleovegetation signals in our records.

#### Implications for Neogene ecosystems of eastern Africa

This study unequivocally extends the record of  $C_4$  grasses in Africa, roughly coeval with

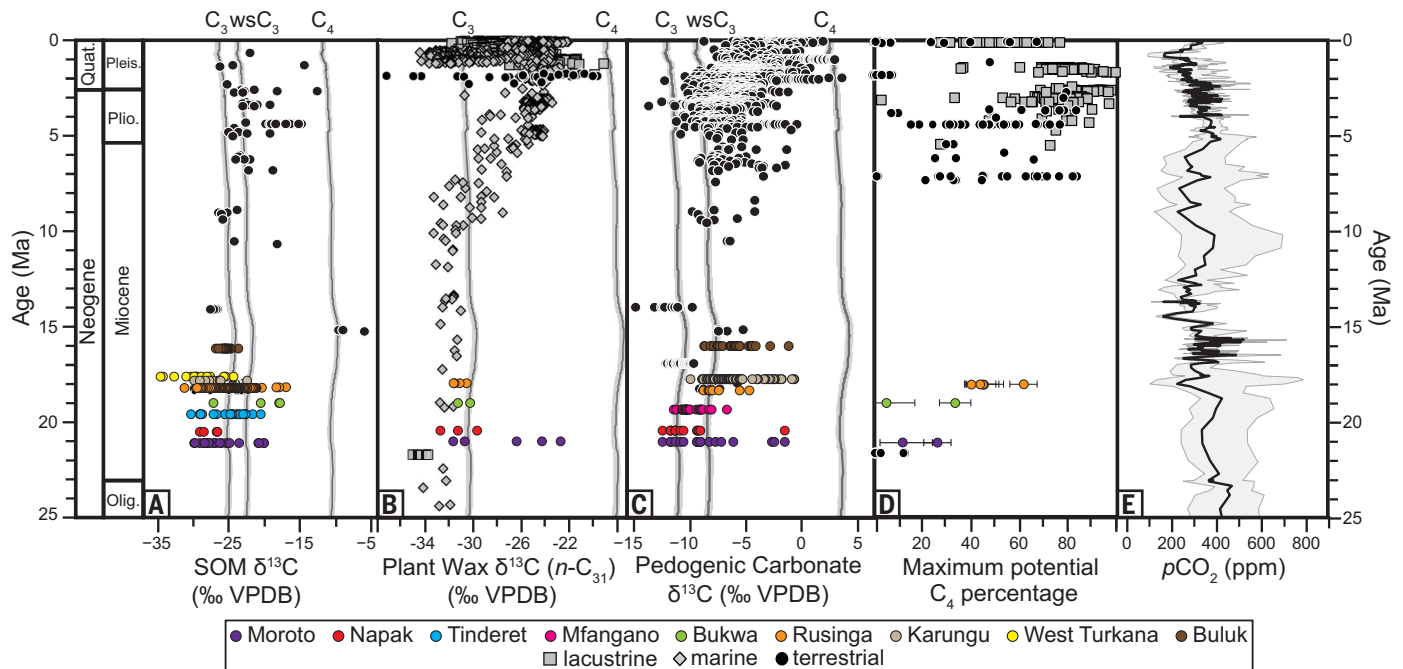


**Fig. 4. Long-term record of isotopes, phytoliths, and  $CO_2$  from the late Oligocene–Holocene for eastern and central Africa.** (A) Soil organic matter (SOM)  $\delta^{13}C$  values from terrestrial samples. (B)  $\delta^{13}C$  values for  $C_{31}$   $n$ -alkane homolog ( $\delta^{13}C_{wax}$ ) from terrestrial, marine, and lacustrine samples. (C)  $\delta^{13}C$  from pedogenic carbonates sampled from paleosols. (D) Maximum potential  $C_4$  (i.e., PACMAD) grass phytoliths of diagnostic counts with 95% confidence bars. (E)  $CO_2$  compilation for the past 25 million years from (29). ppm, parts per million.

Solid line depicts grand mean of all  $CO_2$  proxy data, and gray outline indicates 95% confidence interval. [(A) to (C)] Black lines represent mean  $C_3$ , mean water-stressed ( $wsC_3$ ), and  $C_4$  endmember  $\delta^{13}C$  values calculated and corrected for atmospheric  $CO_2$   $\delta^{13}C$  as for Fig. 2. Data, data sources, and methods are provided in (16), table S1, and data S1, S2, S4, S5, S12, and S13. Quat., Quaternary; Pleis., Pleistocene; Plio., Pliocene; Olig., Oligocene. Holocene not shown owing to the scale of figure.

the earliest records of chloroid phytoliths from North America (3). Furthermore, our data document the occurrence of ecologically abundant and, in several cases, locally dominant C<sub>4</sub> grasses, predating by more than 10 million years the near-global spread of C<sub>4</sub> grasslands in the Late Miocene–Early Pleistocene (Fig. 4) (2, 3). This finding contradicts the longstanding view that C<sub>4</sub> grasses did not gain ecological importance in eastern Africa until the late Neogene (2, 7, 8, 11). Expansion of C<sub>4</sub> grasses has been linked to a range of local to global factors, including decreasing atmospheric pCO<sub>2</sub>, shifts in disturbance regime (e.g., fire, herbivory, volcanism), and changes in regional climate (e.g., aridity, seasonality) (2, 8, 9, 22, 27, 28). However, changes in pCO<sub>2</sub> are not likely to have played a role in structuring Early Miocene vegetation, as CO<sub>2</sub> levels remained relatively high during this time (Fig. 4) (29). Changes in the fire regime and fauna–vegetation interaction may have influenced plant communities, but current evidence from eastern Africa is insufficient to evaluate these hypotheses in the Early Miocene. We hypothesize that regional tectonic factors (e.g., recurrent volcanic eruptions and edifice building, extension-induced formation of escarpments and grabens) expressed variably at the scale of individual sites were the primary controls on heterogeneity and regional C<sub>4</sub> grass dominance in eastern Africa. Orographic climate effects related to doming and uplift associated with incipient rifting would have disrupted both local and regional seasonality and drainage patterns, further enhancing ecological variability. The presence of topographic barriers may also explain the lack of agreement between in situ signals of C<sub>4</sub> vegetation reported in this study and regionally integrated records from marine cores off of the eastern and western coasts of Africa, which first record C<sub>4</sub> signals at 10 Ma (8).

Our discovery that heterogeneously distributed C<sub>4</sub> vegetation preceded the rise to dominance of C<sub>4</sub> grassland habitats in eastern Africa stands in stark contrast to data from North America, South America, Australia, and eastern Asia, which indicate that C<sub>4</sub> grasslands replaced C<sub>3</sub>-dominated grassy mosaics or other open, semiarid to arid vegetation (3, 9, 30). Thus, the C<sub>3</sub>–C<sub>4</sub> transition in eastern Africa may have been more protracted and complex than elsewhere. Additionally, habitat heterogeneity demonstrated by our data counters hypotheses of predominantly forested habitats in the Early Miocene of eastern Africa [(2, 31, 32), but see (33)], instead supporting a more nuanced interpretation of ecosystem evolution (15, 20, 23). At local scales—those at which organisms interact with their environments—the Early Miocene in eastern Africa was characterized by a variety

of habitats, including open vegetation with C<sub>4</sub> grasses. The evident importance of open habitats in the early Neogene compels a deeper time perspective when considering adaptive hypotheses linking mammalian community evolution with grassland expansion in the fossil record.

#### REFERENCES AND NOTES

- R. F. Sage, *New Phytol.* **161**, 341–370 (2004).
- E. J. Edwards et al., *Science* **328**, 587–591 (2010).
- C. A. E. Strömberg, *Annu. Rev. Earth Planet. Sci.* **39**, 517–544 (2011).
- B. Jacobs, J. Kingston, L. Jacobs, *Ann. Mo. Bot. Gard.* **86**, 590–643 (1999).
- J. D. Kingston, in *Late Cenozoic Environments and Hominid Evolution: a tribute to Bill Bishop*, P. Andrews, P. Banham, Eds. (The Geological Society, 1999), pp. 69–84.
- W. E. Lukens et al., *Front. Earth Sci. (Lausanne)* **5**, 87 (2017).
- T. Cerling et al., *Nature* **389**, 153–158 (1997).
- P. J. Polissar, C. Rose, K. T. Uno, S. R. Phelps, P. deMenocal, *Nat. Geosci.* **12**, 657–660 (2019).
- A. T. Karp, A. K. Behrensmeyer, K. H. Freeman, *Proc. Natl. Acad. Sci. U.S.A.* **115**, 12130–12135 (2018).
- S. J. Feakins et al., *Geology* **41**, 295–298 (2013).
- K. T. Uno, P. J. Polissar, K. E. Jackson, P. B. deMenocal, *Proc. Natl. Acad. Sci. U.S.A.* **113**, 6355–6363 (2016).
- K. T. Uno et al., *Proc. Natl. Acad. Sci. U.S.A.* **108**, 6509–6514 (2011).
- N. E. Levin, *Annu. Rev. Earth Planet. Sci.* **43**, 405–429 (2015).
- B. F. Jacobs, A. D. Pan, C. R. Scotese, in *Cenozoic Mammals of Africa*, L. Werdelin, W. J. Sanders, Eds. (Univ. of California Press, 2010), pp. 57–72.
- T. L. P. Couvreur et al., *Biol. Rev. Camb. Philos. Soc.* **96**, 16–51 (2021).
- Materials and methods are available as supplementary materials.
- T. E. Cerling, J. M. Harris, M. G. Leakey, N. Mudida, in *Lothagam: The Dawn of Humanity in Eastern Africa*, M. G. Leakey, J. M. Harris, Eds. (Columbia Univ. Press, 2003), pp. 583–604.
- J. G. Wynn, *Palaeogeogr. Palaeoclimatol. Palaeoecol.* **251**, 437–448 (2007).
- R. T. Bush, F. A. McNerney, *Geochim. Cosmochim. Acta* **117**, 161–179 (2013).
- L. M. MacLachy et al., *Science* **380**, eabq2835 (2023).
- Y. Garcin et al., *Geochim. Cosmochim. Acta* **142**, 482–500 (2014).
- T. E. Cerling, *Global Biogeochem. Cycles* **6**, 307–314 (1992).
- L. A. Michel et al., *Sedimentology* **67**, 3567–3594 (2020).
- M. I. Bird, A. R. Chivas, J. Head, *Nature* **381**, 143–146 (1996).
- A. Novello et al., *J. Hum. Evol.* **106**, 66–83 (2017).
- E. D. Currano et al., *Palaeogeogr. Palaeoclimatol. Palaeoecol.* **539**, 109425 (2020).
- S. Hoetzel, L. Dupont, E. Scheffuß, F. Rommerskirchen, G. Wefer, *Nat. Geosci.* **6**, 1027–1030 (2013).
- P. Sepulchre et al., *Science* **313**, 1419–1423 (2006).
- G. L. Foster, D. L. Royer, D. J. Lunt, *Nat. Commun.* **8**, 14845 (2017).
- C. A. E. Strömberg, R. E. Dunn, C. Crifò, E. B. Harris, in *Methods in Paleocology: Reconstructing Cenozoic Terrestrial Environments and Ecological Communities*, D. A. Croft, D. F. Su, S. W. Stimpson, Eds. (Springer Cham, 2018), pp. 235–287.
- R. J. Morley, K. Richards, *Rev. Palaeobot. Palynol.* **77**, 119–127 (1993).
- S. J. Feakins, P. deMenocal, in *Cenozoic Mammals of Africa*, L. Werdelin, W. J. Sanders, Eds. (Univ. of California Press, 2010), pp. 45–55.
- P. Andrews, *An Ape's View of Human Evolution* (Cambridge Univ. Press, 2015).
- B. H. Passey et al., *J. Geol.* **110**, 123–140 (2002).
- T. E. Cerling et al., *Nature* **476**, 51–56 (2011).
- B. J. Tipler, S. R. Meyers, M. Pagani, *Paleoceanography* **25**, PA3202 (2010).
- D. Peppe et al., Supplementary Data for Oldest evidence of significant C<sub>4</sub> grasses and habitat heterogeneity in eastern Africa, version 1, Texas Data Repository (2023); <https://doi.org/10.18738/T8/TCAMKJ>.

#### ACKNOWLEDGMENTS

This work was conducted under the authority of, and with permits from, the National Commission for Science, Technology, and Innovation (Kenya) and the Department of Museums and Monuments, Ministry of Tourism, Wildlife and Antiquities (Uganda). We thank the staff of the National Museums of Kenya, Turkana Basin Institute, Uganda Museum, and Makerere University for their ongoing research support, with particular thanks to R. Mwanja and J. Kibii. Our gratitude extends to the many collaborators who provided assistance in the field and in museums:

D. Ketch, I. Arney, K. Cheng, J. Erus Edung, S. Ekitela, A. Ekuwom, S. Longoria Eyanee, M. Fuchs, J. Greschbach, C. Hemm, R. Henning, H. Kasozi, J. Kiseu, U. Lächele, M. Macharwas, M. Malone, U. Menz, R. Moru, T. Mukhuyu, B. Nalikka, C. Ochieng, S. Owour Odhiambo, B. Onyango, C. Ouma, T. Rumpf, J. Shaduma, J. Siembo, J. Tausch, and J. Torgeson. T. Cerling graciously provided modern soil samples from eastern Africa from which phytoliths were extracted. This is publication #12 supporting Research on Eastern African Catarrhine and Hominoid Evolution (REACHE). **Funding:** This work was funded by National Science Foundation grant BCS 1241807 (K.P.M. and D.L.F.), National Science Foundation grant BCS 0852609 (K.P.M.), National Science Foundation grant BCS 1241811 (L.M.M.), National Science Foundation grant BCS 1241812 (D.J.P. and S.G.D.), National Science Foundation grant BCS 1241817 (J.B.R.), National Science Foundation grant BCS 1241918 (A.L.D.), National Science Foundation grant EAR 1253713 (C.A.E.S.), National Science Foundation grant EAR 1053549 (B.F.J.), National Science Foundation grant BCS 1638796 (N.J.S.), National Science Foundation grant DGE 16-44869 (S.R.P.), Leakey Foundation grant (K.P.M.), Leakey Foundation grant (N.D.G.), Leakey Foundation grant (K.E.H.J.), Leakey Foundation grant (D.J.P. and K.P.M.), Leakey Foundation grant (L.A.M.), Leakey Foundation grant (E.R.M. and I.O.N.), Leakey Foundation Baldwin Fellowship (K.O.O.), McKnight Land-Grant Fellowship (K.P.M.), National Geographic Society grant (E.R.M. and I.O.N.), Wenner-Gren Foundation Workshop grant (S.M.C., K.P.M., L.M.M., and F.K.M.), Leverhulme Trust Fellowship (K.P.M.), EU Horizon 2020 for Research and Innovation MSCA IOF#659596 (A.N.), Karl und Marie Schack-Stiftung fund (T.L.), Vereinigung von Freunden und Förderern der Goethe-Universität Frankfurt (T.L.), Natural Sciences and Engineering Research Council of Canada (S.M.C.), Tennessee Tech University URECA Program (L.A.M.), Tennessee Tech University Department of Earth Sciences (L.A.M.), Center for Climate and Life, Columbia University (K.T.U.), and Vetlesen Foundation (K.T.U.). **Author contributions:** Conceptualization: S.M.C., A.L.D., S.G.D., D.L.F., J.D.K., L.M.M., F.K.M., E.N.M., K.P.M., A.N., D.J.P., J.B.R., N.J.S., and C.A.E.S. Methodology: S.M.C., S.G.D., D.L.F., J.D.K., R.N.K., K.E.H.J., W.E.L., L.M.M., F.K.M., K.P.M., L.A.M., E.R.M., I.O.N., A.N., K.O.O., D.J.P., S.R.P., P.P. C.A.E.S., and K.T.U. Data analysis: S.G.D., D.L.F., N.D.G., K.R.H., J.D.K., R.N.K., W.E.L., L.A.M., A.N., K.O.O., D.J.P., S.R.P., P.P., C.A.E.S., and K.T.U. Investigation: S.M.C., A.L.D., S.G.D., D.L.F., N.D.G., K.E.H.J., J.D.K., R.N.K., R.M.K., T.L., W.E.L., L.M.M., K.P.M., L.A.M., E.R.M., A.A.T.M., S.N.M., I.O.N., A.N., K.O.O., D.J.P., J.B.R., and C.A.E.S. Funding acquisition: S.M.C., A.L.D., S.G.D., D.L.F., N.D.G., B.F.J., K.E.H.J., J.D.K., T.L., L.M.M., F.K.M., K.P.M., L.A.M., E.R.M., I.O.N., A.N., K.O.O., D.J.P., J.B.R., and C.A.E.S. Project administration: S.M.C., L.M.M., K.P.M., E.R.M., I.O.N., D.J.P., and J.B.R. Writing – original draft: S.M.C., D.L.F., J.D.K., L.M.M., K.P.M., A.N., D.J.P., and C.A.E.S. Writing – review & editing: S.M.C., A.L.D., S.G.D., D.L.F., N.D.G., B.F.J., K.E.H.J., J.D.K., R.N.K., R.M.K., T.L., W.E.L., L.M.M., F.K.M., E.N.M., K.P.M., L.A.M., E.R.M., I.O.N., A.N., D.J.P., S.R.P., P.P., J.B.R., N.J.S., C.A.E.S., and K.T.U.

**Competing interests:** The authors declare that they have no competing interests. **Data and materials availability:** All data are available in the supplementary materials and in the Texas Data Repository online archive (37). **License information:** Copyright © 2023 the authors, some rights reserved; exclusive licensee American Association for the Advancement of Science. No claim to original US government works. <https://www.science.org/about/science-licenses-journal-article-reuse>

#### SUPPLEMENTARY MATERIALS

[science.org/doi/10.1126/science.abq2834](https://science.org/doi/10.1126/science.abq2834)

Materials and Methods

Figs. S1 to S8

Tables S1 to S3

References (38–144)

MDAR Reproducibility Checklist

Data S1 to S13

Submitted 8 April 2022; accepted 10 March 2023  
10.1126/science.abq2834



## Oldest evidence of abundant C<sub>4</sub> grasses and habitat heterogeneity in eastern Africa

Daniel J. Peppe, Susanne M. Cote, Alan L. Deino, David L. Fox, John D. Kingston, Rahab N. Kinyanjui, William E. Lukens, Laura M. MacLatchy, Alice Novello, Caroline A. E. Strmberg, Steven G. Driese, Nicole D. Garrett, Kayla R. Hillis, Bonnie F. Jacobs, Kirsten E. H. Jenkins, Robert M. Kityo, Thomas Lehmann, Fredrick K. Manthi, Emma N. Mbua, Lauren A. Michel, Ellen R. Miller, Amon A. T. Mugume, Samuel N. Muteti, Isaiah O. Nengo, Kennedy O. Oginga, Samuel R. Phelps, Pratifigya Polissar, James B. Rossie, Nancy J. Stevens, Kevin T. Uno, and Kieran P. McNulty

*Science*, **380** (6641), .  
DOI: 10.1126/science.abq2834

### A new habitat for hominoid emergence?

The hominoid lineage underwent a major morphological change in the Miocene, acquiring strong hind legs and a more upright posture. The prevailing hypothesis pertaining to these changes has been that they were adaptive for foraging on fruit in the terminal branches of tropical forest trees. A pair of papers now argue that, instead, such changes may have been driven by adaptation to feeding on leaves in seasonally dry and open forests. Peppe *et al.* used new data from fossil mammal study sites and found that the expansion of grassy biomes dominated by grasses with the C<sub>4</sub> photosynthetic pathway in eastern Africa likely occurred more than 10 million years earlier than prior estimates. MacLatchy *et al.* looked at fossils of the earliest ape in this region at this time, *Morotopithecus*, and found isotope evidence of the consumption of water-stressed vegetation and postcranial morphology indicative of strong hind limbs similar to modern apes. Together, these papers suggest that early hominoids emerged in a dryer and more irregular environment than was previously believed. —BEL and SNV

### View the article online

<https://www.science.org/doi/10.1126/science.abq2834>

### Permissions

<https://www.science.org/help/reprints-and-permissions>

Use of this article is subject to the [Terms of service](#)